

Water-Induced Quenching of Salicylic Anion Fluorescence

Hem C. Joshi, Cees Gooijer, and Gert van der Zwan*

Department of Analytical Chemistry and Applied Spectroscopy, Laser Centre, Vrije Universiteit, De Boelelaan 1083, 1081 HV Amsterdam, The Netherlands

Received: February 18, 2002; In Final Form: July 23, 2002

Salicylic anion absorption and emission are studied in a variety of solvents and solvent mixtures. The large Stokes shift observed for this anion is taken to be indicative of a rapid excited state proton transfer reaction to its keto form. The changes in the Stokes shift in the various solvents can be well-correlated with changes in polarity/polarizability and hydrogen-bonding acidity. The time-resolved data can for the most part also be well-correlated with these properties. A notable exception is the behavior in water and water-rich mixtures. A significant decrease in fluorescence lifetime is observed, and the influence of temperature in pure water is much larger than in other neat liquids. As an explanation for these effects, an excited state intermolecular proton transfer reaction is suggested, from larger-sized water clusters, to the anion.

1. Introduction

About 50 years ago, Weller, in a series of papers on the fluorescence behavior of salicylic acid and methoxy salicylic acid,^{1–3} proposed the existence of an excited state proton transfer reaction between the phenol group and the adjacent carboxyl group, cf. Figure 1, as an explanation for the large Stokes shifts that he observed. His rationale for this phenomenon was that although in the ground state the phenol group is basic and the carboxyl group is acidic, this behavior is reversed in the excited state, and consequently, the proton, which in all likelihood is already close to the carboxyl group due to a rather strong intramolecular hydrogen bond, switches sides. In his papers, he suggests the zwitterionic form (b) of Figure 1 as the resulting compound, which is of course nothing but one of the mesomeric structures related to the keto-tautomer of salicylic acid, depicted in Figure 1c. Because excited state intramolecular proton transfer reactions are thought to be extremely rapid, transfer times faster than 100 fs have been suggested,^{4–6} the possible fluorescence from the primary compound is completely quenched, and only fluorescence from structures b and c will be observed.

Since Weller's publications, a considerable number of papers have been devoted to salicylic acid and its derivatives.^{7–18} Nevertheless, a large number of questions remain unresolved, with respect to both the properties of salicylic acid itself and the more general issue of excited state properties of this and related molecules. Experimentally, the situation is more or less clear. Invariably, a large Stokes-shifted emission is found, at least in condensed phase measurements, and single exponential decay, without ingrowth, supporting the hypothesis that the excited state proton transfer is very rapid, at least faster than 1 ps. Whenever dual emission is reported from salicylic acid, it can always be attributed to the existence of a dimer at higher concentrations,^{10–14} although in a supersonic free jet study dual emission was found by Bisht et al.⁴ and attributed to the presence of both tautomeric forms. Their interpretation of the data assumes the presence of two species in the excited state with rapid, subnanosecond equilibration between them. This is

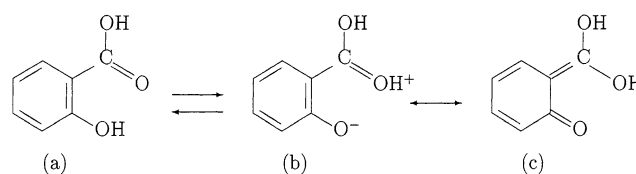


Figure 1. Primary forms of salicylic acid. The enol form (a) is likely the only stable form in the ground state. No observations of the neutral keto form (b,c) have been reported, and theoretical calculations point to the presence of a single well in the ground state at the enol configuration.

consistent with the different vibration excitation spectra detected in the blue and UV region and a single fluorescence relaxation time. It also implies a barrier between these two species and a rather small energy difference between them.

However, theoretical calculations to support Weller's hypothesis of a double well potential for both the ground and the excited state, where the enol form is the most stable in the ground and the keto form is the most stable in the excited state, appear to give contradictory results. Thus, Catalán et al.¹⁹ on the basis of Hartree–Fock/density functional theory (HF/DFT) calculations concluded that the ground state showed a single well at the enol structure and a barrierless transition to a very broad well in the excited state, which extended from a (phenolic) O–H distance of about 1.3 Å, to the point at which they stopped their calculations, at 1.6 Å. The energy of the keto- S_1 state can be estimated from their figures as approximately 10 kcal/mol less than that of the excited enol form. On the other hand, Maheshwari et al.¹⁸ on the basis of ab initio calculations, did find a weak barrier in the excited state, but it appeared that the point at which they put the keto form (≈ 1.8 Å), the energy was actually higher than that of the excited enol form. Ab initio calculations by Sobolewski et al.¹⁷ showed similar excited state energy curves. Neither of these results would explain the very rapid excited state proton transfer reaction, and furthermore, the energy difference found with the first method would be much too large to explain the presence of the enol form in the excited state in any appreciable amount. What is obviously missing in these calculations is the role of the solvent, but even apart from that, it is questionable whether quantum calculations on the

* To whom correspondence should be addressed. E-mail: zwan@chem.vu.nl.

salicylic acid molecule itself will give the answer. In a recent theoretical study on the difference between ground and excited state acidity, in this case in phenol,²⁰ it was concluded that the enhanced acidity of the S_1 state with respect to the S_0 state arises mainly from effects of the deprotonated species, whereas the effects of excitation on conjugated acids are of minor importance.

In solvents, the situation is even less clear. If the interpretation of Bisht et al.¹² is correct, the exceptional behavior in supersonic jets is due to the absence of solvent molecules; in salicylic acid solutions, the excited state keto form is much more stabilized, since in all cases only large Stokes-shifted emission is found. Even though some weak UV fluorescence is found in CCl_4 ,^{13,16} this is attributed to the presence of small amounts of dimer or HCl as an impurity in the solution. On the other hand, it is hard to understand how polar, aprotic media would stabilize the keto form, even if the excited state dipole moment of the keto form is much larger than that of the enol form, for which there is no direct evidence. Although the influence of the solvent on the absorption spectrum is small—hardly any shift of the absorption maximum on changing the solvent properties is detected—the influence on the emission spectra can be considerable. We note here the tendency of salicylic acid to form complexes with certain solvent molecules,¹⁰ and furthermore, the fact that in proton-accepting solvents such as dimethyl sulfoxide (DMSO) or water, emission from the salicylic anion is observed rather than from the neutral molecule.¹⁶ On the basis of fluorometric titration measurements, Denisov et al.¹⁶ also conclude that the $\text{p}K_a$ value is approximately equal to 3.1 both in the ground as well as in the excited S_1 state. Within the context of Weller's conjecture, this would mean that in the ground state the carboxyl group, but in the excited state the phenolic group, is the proton donor. This is consistent with $\text{p}K_a$ values given for naphthol and naphthoic acid and similar compounds, which indeed reverse their acidity in ground and excited state.²¹

For the salicylic anion, the situation is more or less similar to that of salicylic acid. The large Stokes shift is well-documented,²² and in recent years, in both a few experimental and theoretical papers, attention was focused on the photo-physical properties of these anions.^{23,24} It has a higher fluorescence quantum yield than neutral salicylic acid, there is evidence of the presence of the ground state keto form in polar aprotic solvents such as acetonitrile, and no UV fluorescence (indicating the presence of the enol form in the excited state) has been reported.²³ The compound is useful as a sensitizer in UV and VUV detection^{25,26} and in analytical chemistry for sensitizing lanthanide fluorescence.^{27,28}

Friedrich et al.²³ propose the photocycle of the salicylic anion depicted in Figure 2. We will use this scheme as the basis of our investigations as well. In practically all solvents, the ground state equilibrium favors the major tautomer, denoted N, while as indicated above tautomer T can be present in polar aprotic solvents in small amounts. We furthermore note that in the N form, the charge is localized on the COO^- group, whereas in the T form the delocalization is over the complete ring, as indicated in Figure 3. Obviously, the relative contributions of the two forms (or indeed others that can be written down) will be different in the ground and excited state.

In this paper, we further investigate this photocycle in a variety of solvents and solvent mixtures. We are particularly interested in the role of protons present in the medium, to examine the claim by Friedrich et al. that the fluorescence of the T^* state is not inhibited by the possible hydrogen bonding to water or other protic solvents. To that end, we performed a

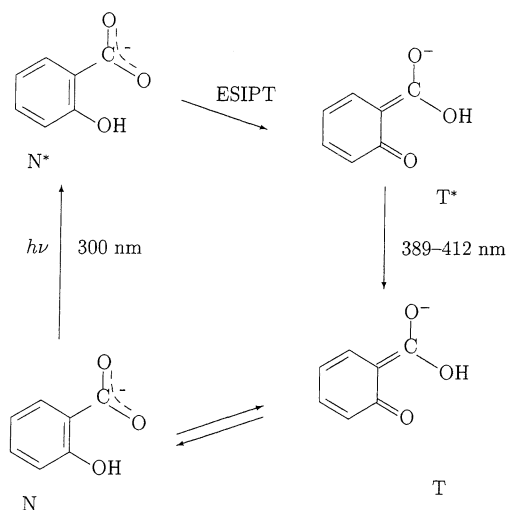


Figure 2. Photocycle of the salicylic anion. The excitation wavelength of the N form is close to 296 nm for all solvents, independent of polarity or proton-donating or -accepting properties. The emission wavelength from T^* varies between 389 nm for hydrogen-accepting solvents (DMSO, DMFA) to 412 nm for proton-donating media (TFE).

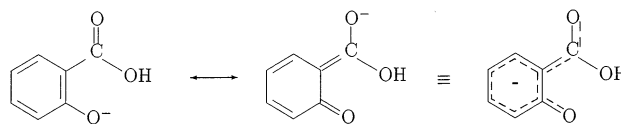


Figure 3. Mesomeric structures of the keto (T) tautomer of the salicylic anion. The charge may be delocalized over the whole ring system, where the relative contributions of these structures is likely different in the ground and excited state.

series of steady state and time-resolved fluorescence measurements of the anion fluorescence in solvents of different polarity and hydrogen-bonding ability and in protic/aprotic solvent mixtures.

Solvent polarity effects can be estimated from the semiempirical calculations (ZINDO) by Friedrich et al.,²³ who also found very small differences in energy between the tautomers in gas phase calculations, but in addition, they gave dipole moments for the various ground and excited states. The ground state dipole moment is slightly larger (6.9 D for the enol vs 5.0 D for the keto form), which would of course make the enol form slightly more stable in polar solvents, but they found only very small changes in dipole moments upon going to the excited state, which does explain the small differences in excitation energies in solvents of different polarity, but it is not in accordance with the much larger stability of the excited state keto form or indeed the very large Stokes shift. The difference in free energy of the two forms can be estimated from the Onsager cavity reaction field expression:²⁹

$$U = -\vec{\mu} \cdot \vec{E}_R = -[2\mu^2(\epsilon - 1)]/[4\pi\epsilon_0 a^3(2\epsilon + 1)] \quad (1.1)$$

In this expression, \vec{E}_R is the reaction field of a dipole $\vec{\mu}$, in a cavity of radius a , in a medium with relative dielectric constant ϵ . Obviously, this only can give a rough estimate, since local structure effects and the cavity radius are hard to estimate, but the difference in free energy between the two forms should at least be an order of magnitude larger than the available energy of $\approx 200 \text{ cm}^{-1}$ (at room temperature) for the keto form to be present in negligible amounts. In the ground state, the dipole moment difference could be just large enough if we assume a cavity radius of approximately 3 Å. It does not, however, explain

why, particularly in highly polar aprotic solvents, the keto form is present and why, in the excited state, the keto form is preferred.

The role of proton-accepting or proton-donating components in the solvents is even harder to reduce to a simple model. In view of the proposed structures and charge distributions of the anionic forms, solvents may form hydrogen bonds at a number of positions—for instance, the phenolic O[−] or the carboxylic oxygens—or even at the center of the aromatic ring itself.³⁰ We will show that there is a definite correlation of the Stokes shift with the hydrogen-bonding ability of solvents, as signified by the hydrogen-bonding donor acidity parameter α .³¹ In addition, the time-resolved measurements show that the fluorescence is quenched in the presence of water and in DMSO/water mixtures; for instance, the fluorescence lifetime decreases from 5.61 ns in pure DMSO to 4.29 ns in pure water, although other strongly proton-donating solvents such as trifluoromethanol (TFE) appear to have almost no effect: a lifetime of 5.58 ns is found. Temperature-dependent measurements of the fluorescence properties in water appear to indicate the presence of an activated quenching mechanism. A state close to the S_1 state lying triplet state¹⁶ or a low-lying singlet $n\pi^*$ state may be responsible for this.^{19,32}

The organization of this paper is as follows. After a section describing experimental details, we first concentrate on an analysis of the Stokes shift data and their dependence on solvent properties. Subsequently, the time-resolved data in the same solvents and mixtures will be presented, as well as temperature-dependent data in pure water. In a separate section, we analyze two possible models to explain the results, favoring the model wherein an additional nonradiative state plays a role. In a separate paper,³³ we describe measurements on substituted salicylic acid, considering both electron-donating and electron-accepting groups at the meta (5-position) and para (4-position) positions of the carboxyl group. Here, we use some of these results to substantiate our findings, however.

2. Experimental Section

Sodium salicylate (Baker Chemicals, Netherlands) was used without further purification. All solvents used, i.e., methanol (MeOH), ethanol (EtOH), 2-propanol (PrOH), ethylene glycol (EG), acetonitrile (ACN), *N,N*-dimethylformamide (DMF), and DMSO, were of spectroscopic grade. 2,2,2-Trifluoroethanol (TFE) was purchased from Aldrich (purity 99+%).

Steady state absorption spectra were recorded on a Cary spectrophotometer, and emission and excitation spectra were recorded on a Perkin-Elmer LS-50 B fluorimeter. For excitation and emission spectra, the optical density of the sample was kept below 0.1 to avoid any inner filter effects. The spectra were automatically corrected for the wavelength dependence of the detector response and the excitation source. Samples were deoxygenated completely by bubbling through dry nitrogen, since oxygen has been found to quench the fluorescence significantly in organic solvents.³⁴ Deoxygenation was performed until the fluorescence intensity did not show a further increase upon continued deoxygenation. Quantum yields φ were determined by using quinine sulfate in 0.5 M H₂SO₄ ($\varphi_{\text{ref}} = 0.546$) as a reference and using the relation³⁵

$$\varphi = \varphi_{\text{ref}} (A_{\text{ref}} I_s n_s^2) / (A_s I_{\text{ref}} n_{\text{ref}}^2) \quad (2.1)$$

In this equation, I_s and I_{ref} are the integrated fluorescence intensities, A_s and A_{ref} are the absorbances, and n_s and n_{ref} are

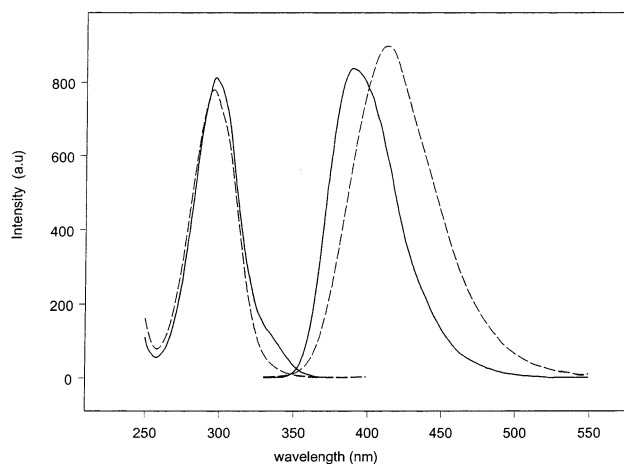


Figure 4. Excitation and emission spectra of the salicylic anion in ACN (drawn lines) and TFE (dashed lines). The small shoulder in ACN at 340 nm is due to the ground state tautomer T. The excitation wavelength for the emission spectra was 300 nm; for the excitation spectra, the emission was recorded at 400 nm.

the refractive indices for the sample and reference, respectively. The accuracy in quantum yield measurements is 5–10%.

Lifetimes were measured using the time-correlated single photon counting technique.³⁶ As the excitation source, a Coherent Mira 900 Ti-sapphire laser was used, which has a pulse width of 3 ps (full width at half-maximum (fwhm)). The output from the laser was frequency-tripled to obtain the exciting wavelength of 295 nm. The energy was ~ 2 nJ/pulse. Fluorescence was collected from the sample through an optical system and dispersed by a spectrometer on a MCP-PMT (Hamamatsu R3809U-50) detector. Decay data were recorded with the help of the SPC-630 (Becker-Hickl) module and analyzed using Fluofit software (Picoquant). In all cases, good single exponential decay fits could be obtained with a reduced χ^2 close to one and residuals distributed randomly. Deconvolution was not deemed necessary for the present measurements since the instrumental response profile was ~ 40 ps and the measured lifetimes were all in the nanosecond range. The accuracy of the instrument was checked by recording the lifetimes of standard compounds. The rms value of deviations for the curves was generally less than 10 ps for each individual measurement. For a series of measurements under the same conditions, the variance was somewhat larger, of the order of 30 ps. In pure water, the variance was larger still (≈ 60 ps, based on 10 measurements), probably due to the larger sensitivity to temperature variations. The temperature was controlled and measured by a home-built system; the accuracy in the temperature measurements was ± 1 K.

3. Results

Steady State Data of the Salicylic Anion in Various Solvents. Fluorescence and excitation spectra of sodium salicylate were measured in a variety of solvents at 296 K. In Figure 4, we show the excitation and emission spectra in two solvents, ACN and TFE, one of which has a small proton-donating capacity (ACN), whereas for the other (TFE) it is large. The excitation spectra are not noticeably different, except for the small shoulder in the excitation spectrum around 340 nm in ACN and other aprotic solvents, which was attributed to the minor tautomer T. The emission spectra have similar shapes but show a markedly different Stokes shift. In Figure 5, we collected a number of emission spectra for water/DMSO mixtures. These

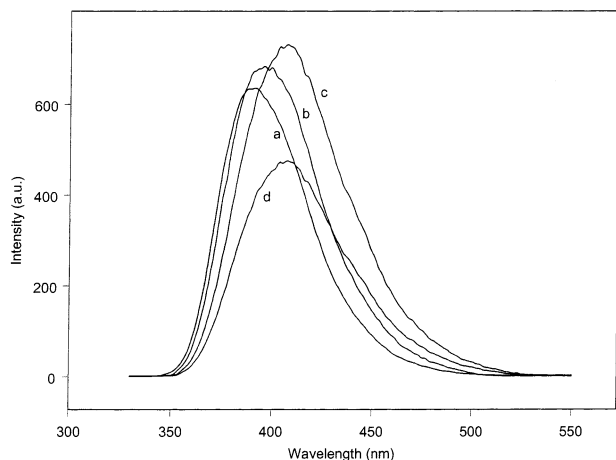


Figure 5. Number of emission spectra from the water/DMSO mixtures. (a) Pure DMSO; (b) $x_{\text{H}_2\text{O}} = 0.496$; (c) $x_{\text{H}_2\text{O}} = 0.940$; (d) pure water. Excitation wavelength was 300 nm. These and the other spectra from the series were used to determine the relative fluorescence quantum yield in water/DMSO mixtures.

TABLE 1: Spectroscopic Data of the Salicylic Anion (2 μM) in Various Solvents at 296 K^a

solvent	$E_{\text{T}}(30)$ (kcal/mol)	π^*	α	β	λ_{abs} (nm)	λ_{em} (nm)	Δ (cm^{-1})	φ	τ_{F} (ns)
DMSO	45	0.98	0.00	0.76	296	391	8208	0.19	5.61
DMFA	43.8	0.88	0.00	0.69	296	389	8077	0.20	5.71
ACN	46	0.73	0.25	0.44	296	389	8077	0.24	6.56
2-PrOH	48.6	0.48	0.76	0.95	296	398	8658	0.23	6.30
EtOH	51.9	0.54	0.83	0.77	297	405	8978	0.25	6.71
EG	56.3	0.88	0.90	0.52	297	406	9039	0.25	6.56
MeOH	55.5	0.60	0.93	0.69	297	405	8978	0.26	6.78
H ₂ O	63.1	1.09	1.17	0.47	296	407	9214	0.16	4.3
TFE	59.5	0.73	1.51	0.00	296	412	9512	0.18	5.58
D ₂ O					296	407	9214	?	5.05

^a The parameters $E_{\text{T}}(30)$, π^* , α , and β are described in the text. λ_{abs} is the absorption maximum, and λ_{em} is the emission maximum, both in nanometers; Δ is the Stokes shift in cm^{-1} ; φ is the quantum yield; and τ_{F} is the fluorescence lifetime in nanoseconds. Solvents are listed in the order of their hydrogen-bonding acidity parameter α , to show the correlation of the Stokes shift with this quantity.

and similar spectra at other concentrations were used to estimate the fluorescence quantum yields reported in Table 2.

To characterize the solvents, we will use the phenomenological scales given by Kamlet and co-workers³⁷ who introduced three dimensionless parameters: the solvent polarity/polarizability π^* , the α - or hydrogen bond donor acidity scale, and the β - or hydrogen bond acceptor basicity scale. These parameters are intended for use as linear solvation energy relationships and should be useful to describe the spectroscopic properties; they are in fact derived from solvatochromic measurements on specified compounds. The parameter π^* should be closely related to the $E_{\text{T}}(30)$ value of Reichardt,³⁸ the Kosower Z values,^{39,40} or the SPP values of Catalán et al.,⁴¹ although in reality the correlation appears to be weak (see also Table 1), which may be indicative of the uncertainties in these parameters. This is also apparent in the values for α that are available from different authors. Marcus⁴² gives data for a variety of solvent mixtures at a number of mole fractions, which we interpolated to get values for the mole fractions used in our experiments. Catalán et al.⁴¹ used a similar scale for water/DMSO mixtures, where their SA scale corresponds to α and SB to β ; the numerical values of these parameters differ only slightly in the few cases where they can be compared. They also allow us to calculate $E_{\text{T}}(30)$ values for these mixtures as a

TABLE 2: Solvent and Photophysical Parameters of the Salicylic Anion (5 μM) in Water/DMSO Mixtures at 300 K^a

$x_{\text{H}_2\text{O}}$	$E_{\text{T}}(30)$ (kcal/mol)	π^*	α	β	λ_{em} (nm)	Δ (cm^{-1})	φ	τ_{F} (ns)
0	45	0.98	0.0	0.76	391	8202	0.19	5.56
0.074	45.7	0.99	0.05	0.78	392	8273		5.63
0.172	46.1	1.00	0.11	0.78	393	8338		5.71
0.304	47.6	1.01	0.20	0.69	394	8403	0.21	5.80
0.496	49.9	1.05	0.32	0.66	397	8595	0.22	5.98
0.628	51.7	1.08	0.40	0.60	401	8846	0.24	6.25
0.724	53.6	1.11	0.49	0.59	402	8908	0.25	6.41
0.797	55.3	1.12	0.59	0.59	404	9031	0.25	6.62
0.855	56.8	1.12	0.70	0.57	405	9092	0.25	6.72
0.902	58.6	1.12	0.82	0.57	406	9153	0.26	6.66
0.940	60.6	1.12	0.94	0.54	407	9214	0.21	6.31
0.972	62.4	1.12	1.06	0.51	408	9274	0.17	5.78
0.986	62.9	1.11	1.12	0.49	408	9274		5.56
0.995	63.1	1.09	1.15	0.48	408	9274		5.31
1.0	63.1	1.09	1.17	0.47	408	9274	0.15	4.1

^a $x_{\text{H}_2\text{O}}$ is the mole fraction of water. $E_{\text{T}}(30)$, π^* , α , and β values were calculated by interpolating the data from ref 42; for $E_{\text{T}}(30)$, a calculation done on the basis of ref 41 gives similar results. Quantum yields were calculated by integrating the spectra to get relative quantum yields for the mixtures and comparing to the independently measured values of DMSO and water from Table 1. The values for pure water differ from those in Table 1 due to the difference in temperature.

TABLE 3: Solvent and Photophysical Parameters of the Salicylic Anion (5 μM) in Water/ACN Mixtures at 300 and 272 K^a

$x_{\text{H}_2\text{O}}$	$E_{\text{T}}(30)$ (kcal/mol)	π^*	α	β	λ_{em} (nm)	Δ (cm^{-1})	τ_{F} (ns) (300 K)	τ_{F} (ns) (272 K)
0.0	46.0	0.73	0.25	0.44	389	8077	6.46	6.72
0.133	51.9	0.76	0.61	0.44	391	8208		6.76
0.245	54.3	0.78	0.74	0.54	392	8273	6.97	7.14
0.422	55.5	0.82	0.84	0.53	398	8658	6.97	7.24
0.556	55.7	0.85	0.88	0.55	401	8846	6.93	7.26
0.661	56.2	0.90	0.91	0.56	403	8970	7.02	7.28
0.745	57.0	0.94	0.93	0.56	404	9031	6.89	6.78
0.814	57.8	0.98	0.97	0.56	404	9031	6.52	6.93
0.872	58.9	1.04	1.02	0.56	405	9092	6.93	7.28
0.921	60.6	1.10	1.07	0.55	406	9153	6.50	6.99
0.963	62.5	1.10	1.12	0.50	408	9274	6.12	5.95
0.982	63.1	1.09	1.15	0.49	408	9274	5.35	5.72
1.0	63.1	1.09	1.17	0.47	408	9274	4.16	5.35

^a For the other parameters, cf. the caption of Table 2.

function of the mole fraction, leading to similar results as those based on Marcus' data.

Because the absorption spectrum of the salicylic anion depends very little on any of these parameters, the susceptibility for a changing environment—mainly determined by the difference dipole moment of the molecule—must be small. This is in line with the calculations of Friedrich et al.,²³ who give a value of 0.148 D for the N form. The T form has a bigger change in difference dipole moment (≈ 1 D), which can be taken as indicative for larger changes in the electronic structure upon excitation, and hence a larger susceptibility for environmental parameters, observed as variations in the Stokes shift.

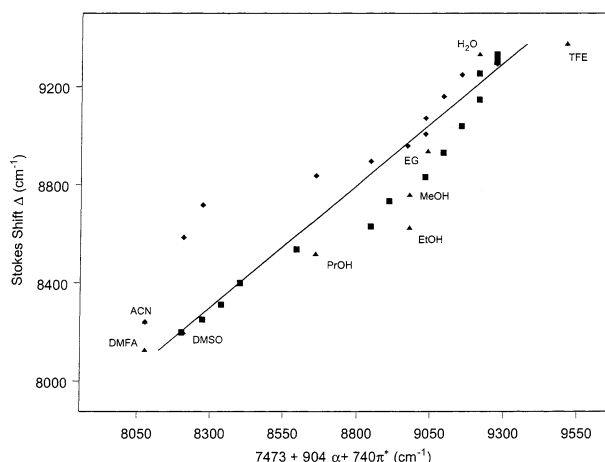
Spectroscopic data for the pure solvents are collected in Table 1, together with solvent parameters taken from refs 37, 38, and 42; in general, we took the values that were published most recently for a particular solvent or for which there appears to be more consensus. Spectroscopic data for the mixtures are collected in Tables 2–5, together with interpolated values for the Kamlet–Taft parameters.

At first glance, the Stokes shift appears to be well-correlated with the ability of the solvent to form hydrogen bonds: the larger α , the bigger the Stokes shift. A linear regression analysis

TABLE 4: Solvent Parameters and Lifetimes of the Salicylic Anion (5 μ M) in Water/MeOH Mixtures at 300 K^a

$x_{\text{H}_2\text{O}}$	$E_T(30)$ (kcal/mol)	π^*	α	β	τ_F (ns)
0.0	55.5	0.60	0.93	0.69	6.94
0.106	55.8	0.67	1.01	0.69	6.90
0.2	56.1	0.72	1.01	0.67	6.87
0.36	56.7	0.82	0.99	0.67	6.86
0.491	57.3	0.90	0.98	0.70	6.78
0.600	57.8	0.97	0.98	0.69	6.57
0.693	58.4	1.02	1.01	0.66	6.10
0.771	59.2	1.07	1.03	0.63	5.89
0.840	60.0	1.11	1.05	0.58	5.43
0.906	61.1	1.12	1.12	0.54	5.01
0.953	62.4	1.09	1.20	0.53	4.80
1.0	63.1	1.09	1.17	0.47	4.10

^a The change in emission wavelength is small in this case: from 405 nm in pure MeOH to 408 nm in pure water.

**Figure 6.** Solid line, Stokes shift data fitted vs eq 3.1; different pure solvents, triangles; water/DMSO mixtures, squares; water/ACN mixtures, diamonds.

without taking β into account gives for the relation between the Stokes shift Δ and the independent parameters α and π^*

$$\Delta = (7473 \pm 147) + (904 \pm 65)\alpha + (740 \pm 149)\pi^* \quad (3.1)$$

The cross-correlation between α and π^* is small (0.1). If we also take β into account, the fit is only marginally better, with a small coefficient and a large error in the β contribution, suggesting that the influence of β on the Stokes shift is rather small. This could be expected since the available hydrogen of the salicylic anion is tied up in an internal hydrogen bond strong enough to withstand even the solvent with high values of β . In Figure 6, the results of the fit are shown, together with all available data points. It should be noted that the DMSO/water mixture data points are all rather close to the fitted values (solid line in Figure 6), whereas ACN/water shows large deviations, especially for the smaller Stokes shifts (low water concentrations).

To fit this relation, we used all of the data available to us, both on the pure solvents and on the mixtures. We also performed regression analyses on the solvent mixtures separately,

where we found that the DMSO/water mixtures give a slightly better fit when just fitted with α

$$\Delta = (8314 \pm 54) + (918 \pm 73)\alpha \quad (3.2)$$

Taking β and π^* into account in this case leads to contributions of these parameters with a relative error of more than 100% and no better overall fit. For the contribution of π^* , this is not surprising in view of the small variation of this parameter in these mixtures, for β the same observation made earlier still holds. No significantly better fits were obtained just using the ACN/water data. Equations 3.1 and 3.2 are consistent: for water/DMSO mixtures, the value of π^* is close to one, and adding 740 to 7473 (eq 3.1) gives 8314 (eq 3.2) within the error margins given.

Using $E_T(30)$ as the polarization parameter rather than π^* , similar results were obtained. This is not surprising since $E_T(30)$ can be written to a good approximation as a linear combination of α and π^* .⁴²

It should be emphasized that not too much value should be given to the precise value of the fit parameters, mainly since they are purely phenomenological; the exact values have still not really settled, and the physical basis, especially for α and β , is not really well-founded. Furthermore, it is clear that parameters such as α and π^* are in general not mutually independent, usually nonzero cross-correlations are found in the fitting procedures, but even apart from that, it is clear that polarizability must have some influence on the position of the equilibrium for a proton dissociation of a solvent molecule. Nevertheless, we feel it is safe to draw the conclusion from our results that the parameter β , measuring proton-accepting properties of the solvent, is of minor or no influence on the Stokes shift, which because the emission wavelength is practically the same for all solvents used, can directly be related to the energy difference between ground and excited state of the keto form. On the basis of both the results for all solvents and separately those for DMSO/water, we can also conclude that both the polarizability of the medium and the acidity play a role in stabilizing the excited state of the keto form. For the polarizability, this should not be really surprising in view of the difference in dipole moments between the ground and the excited state, although the factor $(\epsilon - 1)/(2\epsilon + 1)$, cf. eq 1.1, varies only little for all of the polar solvents that we use, but local structure around the anion, or indeed differences in cavity size in different solvents, are also relevant.

There is currently no theory available for which molecular property is responsible for its susceptibility to a proton-donating environment, which relates the amount of hydrogen bonding to the energy of the state that the hydrogen is bonded to. It is obvious that increased hydrogen-bonding capacity of the solvent lowers the energy of the molecule, however, which thus gives a large Stokes shift in cases of high α .

Finally, from the fact that the Stokes shift can be fitted reasonably well with this procedure, after all relative errors are all less than 10%, it can be concluded that none of the solvents behave strikingly different with respect to this probe as far as static properties are concerned. This is different from the time-resolved behavior discussed below.

TABLE 5: Fluorescence Lifetime of the Salicylic Anion (5 μ M) in Water/TFE Mixtures at 300 K as a Function of the Mole Fraction of Water^a

$x_{\text{H}_2\text{O}}$	0	0.176	0.310	0.503	0.634	0.730	0.802	0.858	0.904	0.942	0.987	1
τ_F (ns)	5.59	5.63	5.60	5.59	5.57	5.56	5.47	5.37	5.0	4.81	4.47	4.1

^a Solvent parameters are not available for these mixtures. The emission wavelength varies from 408 nm for pure water to 412 nm for pure TFE in an almost linear fashion.

Time-Resolved Measurements in Pure Solvents and in Mixtures. Fluorescence decay times were measured in all of the pure solvents mentioned in the Experimental Section, as well as in mixtures of DMSO/water, ACN/water, MeOH/water, and TFE/water. Our main aim was to investigate the dependence of the fluorescence relaxation times on the proton-donating capacities of the solvent.

We found no dependence of the fluorescence relaxation times on the excitation or the emission wavelength of the system. It is important to realize that in organic solvents quenching by oxygen can shorten the fluorescence lifetimes; probably the small value (4.8 ns) measured by Friedrich et al.²³ must be attributed to a nondeoxygenated sample. We also found that in air-saturated samples the lifetime is 4.81 ns, whereas under a nitrogen atmosphere the lifetime increased to 6.56 ns, whereas under pure oxygen it decreased to 2.72 ns. The oxygen concentration was given by Wilkinson and co-workers⁴³ to be 1.9×10^{-3} M in air-saturated ACN. From this value, and our measurements, the quenching constant for oxygen quenching can be estimated to be

$$k_q = \frac{\tau^{-1} - \tau_{N_2}^{-1}}{[O_2]} \approx 2.9 \times 10^{10} \text{ M}^{-1} \text{ s}^{-1} \quad (3.3)$$

where τ_{N_2} is the lifetime under pure nitrogen and τ is the lifetime under other conditions. This is close to the k_q value reported ($1.5 \times 10^{10} \text{ M}^{-1} \text{ s}^{-1}$) by Boscá et al.³⁴ for similar measurements in MeOH. The short lifetimes (3.6 ns) reported by Smith and Kaufmann in MeOH⁷ could also be due to this effect, although at the concentrations they used (10^{-3} M) dimerization could also have played a role.

Lifetimes and quantum yields in a number of solvents are reported in Table 1 for pure solvents and Tables 2–5 for the solvent solvent mixtures. It is interesting to note that lifetimes show very little variation between solvents and only minor variation with temperature, with the exception of water. Both very strong hydrogen-accepting solvents (DMSO) and hydrogen-donating solvents (TFE) give very similar fluorescence lifetimes.

For the pure solvents, we also determined the quantum yields. For the DMSO/water mixtures, we determined relative quantum yields by comparing the spectral areas and relating them to the measurements on the pure solvents. For a single-exponential process, the ratio of the fluorescence lifetime τ_F to the quantum yield φ should be constant. This is remarkably well-satisfied by our measurements. The average intrinsic fluorescence lifetime τ_0 is given by

$$\tau_0 = \langle \tau_F \varphi \rangle = 28(\pm 3) \text{ ns} \quad (3.4)$$

The error is close to the 5–10% error in the quantum yields. Water, with the shortest lifetime, gives 26.9 ns, which is close to the average value.

All solvent mixtures show similar behavior if the water concentration is increased. In Figure 7, the relaxation rates (inverse relaxation times) are plotted as a function of the mole fractions of water in the solvent mixtures investigated. Up to water mole fractions of about 0.8, the behavior is gradual in all cases, almost flat in the case of TFE and ACN, a gradual increase in the case of MeOH and a gradual decrease in the case of DMSO. Noteworthy, in all cases, we see a sharp increase of the relaxation rate at higher mole fractions of water. In ACN, there is also a minor feature at mole fractions around 0.7–0.9. Since in earlier work^{44,45} on dielectric and thermodynamic properties of water/ACN mixtures special features in that region

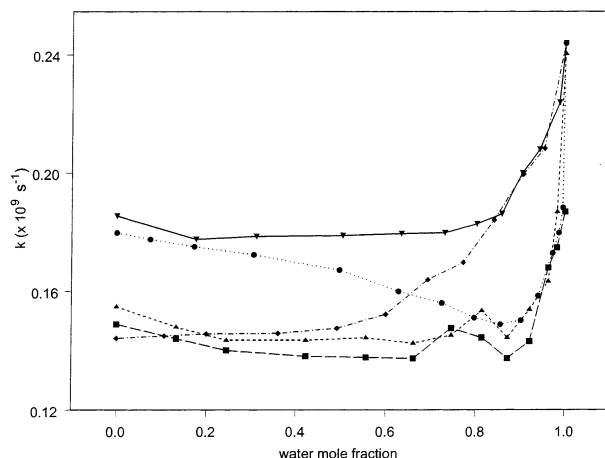


Figure 7. Fluorescence relaxation rates k for the salicylic anion in water–cosolvent mixtures as a function of the water mole fraction. Upside down triangles and drawn line, TFE/water; circles and dotted line, DMSO/water; diamonds and dot-dashed line, MeOH/water; triangles and short dashes, ACN/water at 272 K; squares and long dashes, ACN/water at 300 K.

were identified as possibly due to the existence of a critical demixing point at a mole fraction of 0.7 and a temperature of 270 K, we performed additional lifetime measurements at a lower temperature, which shows the same behavior but does not show a marked increase of this feature as in the case of, for instance, the dielectric behavior or the enthalpy of solvation of tetraalkylammonium salts.

The above measurements suggest the existence of an additional quenching mechanism in water, or in mixtures with a high water concentration, at mole fractions higher than 0.8. To study this further, we also performed a series of lifetime measurements at different temperatures. In Table 6 and Figure 8, we report the results of this study. The data points can be fitted rather well with the following expression based on the assumption that the additional quenching process is a barrier transition

$$k = k_{T=0} + k_{H_2O} e^{-E_a/RT} \quad (3.5)$$

Here, k is the measured rate, $k_{T=0}$ is the rate in absence of additional water quenching, E_a is an activation energy, and k_{H_2O} is the water-quenching rate, which could be decomposed in a diffusional and barrier component, but the number of data points and the range of temperatures do not warrant such a decomposition.

The fitted values of the various constants are

$$k_{T=0} = 1.4 \times 10^{10} \text{ s}^{-1}, \tau_{T=0} = 7.3 \text{ ns} \quad (3.6)$$

which is the relaxation time in the absence of the additional quenching process (at $T = 0$). Furthermore,

$$k_{H_2O} = 1.72 \times 10^{13} \text{ s}^{-1}, \tau_{H_2O} = 60 \text{ fs} \quad (3.7)$$

which is the rate at very high temperatures, when the water-quenching process is dominant; finally, the activation energy is given by

$$E_a = 4.4 \text{ kcal/mol} \quad (3.8)$$

Because the proton transfer frequency is very high, the results of the fit give a high barrier as well. Obviously, we cannot put too much value on these numbers as such in view of the rather

TABLE 6: Fluorescence Lifetimes of the Salicylic Anion (5 μM) in Water as a Function of Temperature^a

temperature (K)	272	278	283	293	298	300	303	313	323
τ_F (ns)	5.35	5.13	4.95	4.56	4.29	4.16	3.95	3.56	3.22

^a Excitation wavelength 300 nm; emission detected at 405 nm.

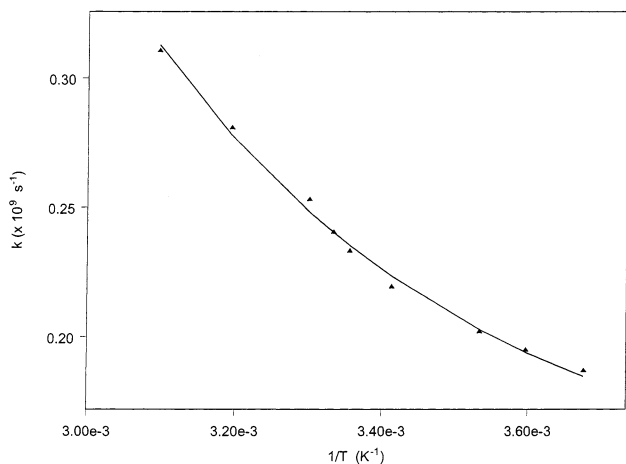


Figure 8. Fluorescence relaxation rates k in water as a function of the inverse temperature ($1/T$). The drawn line is the fitted expression (3.5); data points are triangles.

limited temperature range that we were able to study, but the limiting proton transfer time is well within the range of that of excited state proton transfers, and the data are consistent with the model to a rather high degree (residues distributed normally, with residual standard error 0.003; relative standard errors in the coefficients less than 10%; all additional data fitting was performed with the S-PLUS statistical package).

4. Discussion

The fluorescence and fluorescence-quenching behavior does, in almost all cases, not show exceptional behavior. The fits of the Stokes shift data show that a linear model with the three Kamlet parameters is satisfactory, although the ACN/water mixtures show noticeable deviations.

It is clear from the data in Table 1 that the equilibrium parameters such as acidity and polarity have little influence on the fluorescence relaxation times. This is not surprising since these parameters are basically equilibrium quantities, whereas the dynamics is governed by other dynamical solvent parameters, such as viscosity or dielectric relaxation times.

A conspicuous exception to this is the fluorescence quenching in pure water or in water-rich mixtures. Some of the data clearly point to an additional quenching process in the presence of water, albeit not in other proton-donating solvents: in pure TFE, for instance, the fluorescence rate is virtually identical to that in pure DMSO, and in most alcohols, the lifetimes are rather long. On the other hand, the proposed acidity of the salicylic anion in the excited state ($\text{p}K_a = 3.1^{16}$) does not allow a proton transfer to this state. The possibility of nearby other states can, however, not be excluded. A close-lying triplet state could be responsible, but triplet states usually have an acidity very similar to that of the ground state.²¹ An alternative, which has already been proposed for molecules such as salicylic acid by ref 32 could be a low-lying $n\pi^*$ singlet state. This could explain most of the behavior observed: upon excitation, the proton is rapidly transferred from the phenol to the carboxyl group, resulting in the keto form of the ion, as indicated in Figure 2. Larger values of α and/or π^* result in a larger Stokes shift, due to stabilization of the ion, and also an increased lifetime and quantum yield.

This can be seen most clearly from the DMSO/water data, where π^* is almost constant, and α increases steadily, as do the Stokes shift and lifetime. If a low-lying $n\pi^*$ state is present, the larger Stokes shift observed when increasing the water fraction would bring it within reach of the original excited state, and additionally, sufficient clustered water molecules become available for a proton transfer to this new state to take place. Similar behavior is observed for the other water/cosolvent mixtures. It is unfortunate that solvent parameters are not known for TFE/water mixtures, although the decrease in π^* and the concurrent increase in α could result in the insensitivity of τ_F to the mole fraction of water up to 0.8. Finally, upon protonation, the $n\pi^*$ decays to the ground state, where it is eventually deprotonated again and converted to the enol form.

There is one potential problem with this model, which we now investigate. The rate by which the proposed $n\pi^*$ state is protonated should affect the fluorescence rate of the T^* state. This is possible if the back reaction from the $n\pi^*$ state to the T^* state is significant. A simple model calculation, given in Appendix A, shows that the population of the T^* state as a function of time t can be written as

$$n_{T^*}(t) = n_{T^*}(0) \frac{s_1 + k + k_-}{s_1 - s_2} e^{s_1 t} + n_{T^*}(0) \frac{s_2 + k + k_-}{s_2 - s_1} e^{s_2 t} \quad (4.1)$$

with

$$s_{1,2} = (1/2) [- (k + k_- + k_+ + k_F) \pm \sqrt{(k + k_- - k_+ - k_F)^2 + 4k_+k_-}] \quad (4.2)$$

In this expression, k_F is the fluorescence rate of the T^* state in the absence of other processes. The rate k_+ is the forward rate to state $n\pi^*$, and k_- is the reverse rate. Finally, the rate k is the rate by which the $n\pi^*$ state is taken away, which can be identified with the proton transfer rate.

If we take the limit $k_- \rightarrow 0$, expression 4.1 reduces to

$$n_{T^*}(t) = n_{T^*}(0) e^{-(k_F + k_+)t} \quad (4.3)$$

which shows that indeed a faster proton transfer rate to the $n\pi^*$ state is of no influence to the fluorescence behavior of the T^* state. Obviously, k_+ cannot by itself refer to the proton transfer process; this would contradict the observations made earlier regarding the acidity of the excited keto state. For the new state to influence the T^* state, we need a reverse reaction, which becomes available once the energy of the T^* state is low enough. However, this has the side effect that double exponential decay results, as can be inferred from eq 4.1.

If we expand eq 4.2 for small values of the reverse rate, the rate in eq 4.3 changes to

$$k_F + k_+ + \frac{k_+k_-}{k_+ + k_F - k} \approx k_F + k_+ + \frac{k_+k_-}{k_+ + k_F} + k \frac{k_+k_-}{(k_+ + k_-)^2} \quad (4.4)$$

Obviously, an equally good fit of the data can be obtained using this expression, although now it is of course not as easy to identify the fitting parameters directly with individual rates. The

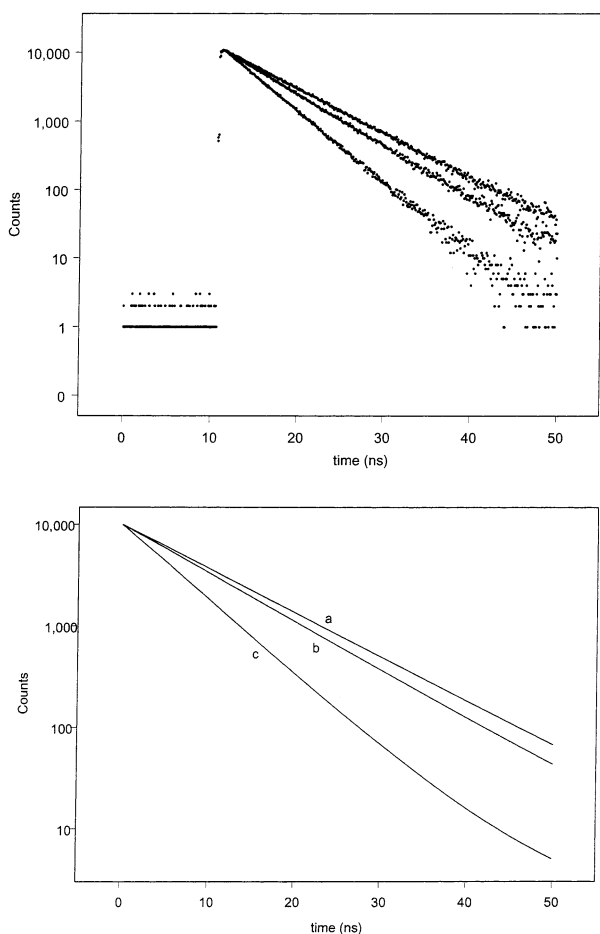


Figure 9. (a) Measured fluorescence decay traces of 5 μM sodium salicylate in water/DMSO mixtures. From top to bottom: $x_{\text{H}_2\text{O}} = 0.902$, $x_{\text{H}_2\text{O}} = 0.972$, and pure water. Excitation wavelength 295 nm, detection at 400 nm. (b) Modeled fluorescence traces using eq 4.1. (a) $k_{\text{F}} = 0.05 \text{ ns}^{-1}$, $k_{\text{r}} = 0.16 \text{ ns}^{-1}$, $k_{\text{r}} = 0$; (b) $k_{\text{F}} = 0.05 \text{ ns}^{-1}$, $k_{\text{r}} = 0.21 \text{ ns}^{-1}$, $k_{\text{r}} = 0.001 \text{ ns}^{-1}$, $k = 0.01 \text{ ns}^{-1}$; (c) $k_{\text{F}} = 0.05 \text{ ns}^{-1}$, $k_{\text{r}} = 0.35 \text{ ns}^{-1}$, $k_{\text{r}} = 0.005 \text{ ns}^{-1}$, $k = 0.1 \text{ ns}^{-1}$.

model is consistent in the sense that the second relaxation time that would show up in eq 4.1 is long, with a small prefactor, so that the relaxation behavior still looks single exponential. The number of data points and the range of temperatures over which the measurements could be taken do not warrant the use of the full expression 4.1 for fitting. In Figure 9b, some model calculations are shown, based on eq 4.1. Although not intended as a fit, it shows conclusively that for reasonable values of the parameters, the decay is to a very good approximation single exponential; only for long times, when the photon count is below 100, deviations become apparent. The experimental data do not allow us to draw any clear conclusions (cf. Figure 9a) for such low photon counts. Parameters for the curves were chosen such that the lifetimes and quantum yields are more or less reproduced. The solutions given are not unique; other parameter values yield similar results, but they are consistent with the ideas presented in the text. In the modeling calculations, we also adapted the ratio k_{+}/k_{-} to reflect the change in equilibrium constant between the T* and the $n\pi^*$ state when the $n\pi^*$ comes closer in energy.

It is apparent that the water content of the solvent plays a crucial role in the quenching mechanism. In a recent paper,⁴⁶ proton transfer from 5-cyano-2-naphthol, which can lose the phenolic proton upon excitation, was studied in water/MeOH mixtures. The time-resolved fluorescence data were interpreted

within the context of a proton transfer to water clusters, where the cluster size turns out to be important.^{47,48} The mechanism proposed by us would be the inverse of this: water clusters of large enough size are capable of donating a proton to an as yet unidentified state of the excited salicylic anion. Similar quenching behavior was also seen in 1-naphthol and 2-naphthol,⁴⁹ 2-anilinonaphthalene,⁴⁷ and aminonaphthalimide derivatives.⁵⁰ Because almost all organic solvents break the water structure,⁵¹ a critical water mole fraction of about 0.8 can be identified above which proton transfer becomes possible. The fluorescence data in ACN/water mixtures around a mole fraction of 0.7 could be taken as additional proof (albeit slim) of this mechanism, since in these mixtures the formation of water clusters around solvent molecules was suggested earlier as an explanation of thermodynamic and dielectric relaxation data.^{44,45}

On the basis of the papers by Robinson et al.,^{47,48} we can make an estimate of the cluster size needed. On the basis of Figure 7, we see an increase of the overall rate of about 40–60%. Comparison with Figures 4 and 5 of ref 48, especially the lower temperature data points, shows that in our case the cluster size should also be around four water molecules. In some cases, most notably in DMSO/water mixtures, we also find a small decrease in the overall fluorescence rate. An explanation could be that the excited salicylate anion is slightly stabilized by an increased hydrogen bonding to the solvent, although the model calculations of ref 48 also show this minor decrease.

Some further evidence can be found from the investigation of substituted salicylic acids, which we report on more extensively in a separate paper.³³ With substitution of the electron-donating methoxy group in the 5-position, the quenching becomes more pronounced, whereas substitution of the electron-withdrawing chloro- and SO_3^- group at the same position substantially reduces the quenching by water. These observations point to a larger (in the methoxy case) or smaller (for SO_3^-) susceptibility of the resulting molecule for intermolecular proton transfer, where the reason can be found in the lower, respectively, higher electron density on the phenolic or carboxylic oxygens, which affects the energy difference between the T state and the $n\pi^*$ state and thus the influence of the latter.

5. Concluding Remarks

The photophysical behavior of the salicylic anion and its solvent dependence is still not completely understood. Most of the static properties, such as absorption and emission, show a clear correlation with solvent properties, as do most of the time-resolved data. Water, either in its pure form or at high concentrations in solvent mixtures, appears to have a specific influence on the fluorescence lifetime, which suggests the presence of an excited state intermolecular proton transfer. This is—at least in the solvents investigated—limited to water, even highly acidic solvents such as TFE do not show an appreciable change with temperature for instance, although the lifetimes are somewhat shorter than in less acidic solvents, such as alcohols. An additional example can be found in EtOH, where we measured the fluorescence lifetime of the salicylic anion in the glass phase at 98 K: the lifetime increases only from 6.71 ns at room temperature to 7.66 ns, which shows that the contributions from other nonradiative pathways are rather insensitive to temperature changes.

Stabilization of the salicylic anion through the formation of hydrogen bonds with water molecules can of course be easily rationalized. An excited state intermolecular proton transfer to produce the neutral keto form of the molecule cannot be understood so easily. Although the data presented here are not

inconsistent with an activated mechanism, the acidity of the excited molecule should preclude this direct mechanism. We have shown that a mechanism where an additional, nonradiative state plays a role can be helpful in interpreting the data, but the number of parameters required and the necessarily limited data set do not allow us to give unambiguous proof that such a state is involved. The behavior found in water/ACN mixtures supports the model. Possibly, pump-probe measurements on a femto-second time scale could be of help in demonstrating the presence of such a state.

Appendix

In this appendix, we give a brief derivation of the model described in the text, leading to eqs 4.1 and 4.2. The number of T* molecules, $n_{T^*}(t)$, satisfies the following equation:

$$\frac{dn_{T^*}(t)}{dt} = - (k_F + k_+)n_{T^*}(t) + k_-n_{n\pi^*}(t) \quad (1)$$

In this equation, k_F is the fluorescence rate of T* in the absence of the presumed $n\pi^*$ state, which includes both fluorescence and possible other nonradiative decay paths. The forward rate k_+ is the rate with which T* molecules are converted to the $n\pi^*$ state, and the reverse rate k_- is the rate of back conversion of the $n\pi^*$ state to the T* state.

Similarly, the number of molecules in the $n\pi^*$ state at time t , $n_{n\pi^*}(t)$, is given by the equation

$$\frac{dn_{n\pi^*}(t)}{dt} = - (k + k_-)n_{n\pi^*}(t) + k_+n_{T^*}(t) \quad (2)$$

where k is the rate for an activated process (the presumed proton transfer to water clusters) by which molecules in the $n\pi^*$ state can also be lost, in addition to the back conversion to T*.

These two coupled linear equations can easily be solved using standard methods. The eigenvalues of the dynamic matrix

$$\begin{pmatrix} - (k_F + k_+) & k_- \\ k_+ & - (k + k_-) \end{pmatrix} \quad (3)$$

are given in the main text as $s_{1,2}$, eq 4.2. The general solution of the equations can then directly be found as

$$n_{T^*}(t) = Ae^{s_1 t} + Be^{s_2 t} \quad (4)$$

where A and B are coefficients that can be found by using the initial conditions, where we assumed that initially no molecules were present in the $n\pi^*$ state.

References and Notes

- Weller, A. *Naturwissenschaften* **1955**, *42*, 175.
- Weller, A. Z. *Elektrochem.* **1956**, *60*, 1144.
- Weller, A. *Prog. React. Kinet.* **1961**, *1*, 187.
- Bisht, P. B.; Petek, H.; Yoshihara, K.; Nagashimi, U. *J. Chem. Phys.* **1995**, *103*, 5290.
- Lochbrunner, S.; Wurzer, A. J.; Riedel, E. *J. Chem. Phys.* **2000**, *112*, 10699.
- Bader, A. N.; Ariese, F.; Gooijer, C. *J. Phys. Chem. A* **2002**, *106*, 2844.
- Smith, K. K.; Kaufman, K. J. *J. Phys. Chem.* **1978**, *82*, 2286.
- Smith, K. K.; Kaufman, K. J. *J. Phys. Chem.* **1981**, *85*, 2895.
- Acuña, A. U.; Catalán, J.; Toribio, F. *J. Phys. Chem.* **1981**, *85*, 241.
- Joshi, H. C.; Tripathi, H. B.; Pant, T. C.; Pant, D. D. *Chem. Phys. Lett.* **1990**, *173*, 83.
- Pant, D. D.; Joshi, H. C.; Bisht, P. B.; Tripathi, H. B. *Chem. Phys.* **1994**, *185*, 137.
- Bisht, P. B.; Tripathi, H. B.; Pant, D. D. *J. Photochem. Photobiol. A* **1995**, *90*, 103.
- Denisov, G. S.; Golubev, N. S.; Schreiber, V. M.; Shajakhmedov, Sh. S.; Shurukhina, A. V. *J. Mol. Struct.* **1996**, *381*, 73.
- Joshi, H. C.; Mishra, H.; Tripathi, H. B. *J. Photochem. Photobiol. A* **1997**, *105*, 15.
- Lahmani, F.; Zehnacker-Rentien, A. *J. Phys. Chem. A* **1997**, *101*, 6141.
- Denisov, G. S.; Golubev, N. S.; Schreiber, V. M.; Shajakhmedov, Sh. S.; Shurukhina, A. V. *J. Mol. Struct.* **1997**, *436*, 153.
- Sobolewski, A. L.; Domcke, W. *Chem. Phys.* **1998**, *232*, 257.
- Maheshwari, S.; Chowdhury, A.; Sathyamurthy, N.; Mishra, H.; Tripathi, H. B.; Panda, M.; Chandrasekhar, J. *J. Phys. Chem. A* **1999**, *103*, 6257.
- Catalán, J.; Palomar, J.; de Paz, J. L. G. *J. Phys. Chem. A* **1997**, *101*, 7914.
- Granucci, G.; Hynes, J. T.; Millié, P.; Tran-Thi, T.-H. *J. Am. Chem. Soc.* **2000**, *122*, 12243.
- Bartrop, J. A.; Coyle, J. D. *Principles of Photochemistry*; John Wiley & Sons: New York, 1978.
- Berlman, I. B. *Handbook of Fluorescence Spectra of Aromatic Molecules*; Academic Press: New York, 1997.
- Friedrich, D. M.; Wang, Z.; Joly, A. G.; Peterson, K. A.; Callis, P. R. *J. Phys. Chem. A* **1999**, *103*, 9644.
- Wang, Z.; Friedrich, D. M.; Ainsworth, C. C.; Hemmer, S. L.; Joly, A. G.; Beversluis, M. R. *J. Phys. Chem. A* **2001**, *105*, 942.
- Bruner, E. C., Jr. *J. Opt. Soc. Am.* **1969**, *59*, 204.
- Butner, C. L.; Viehmann, W. *Appl. Opt.* **1984**, *23*, 2046.
- Schreurs, M.; Gooijer, C.; Velthorst, N. *Anal. Chem.* **1991**, *62*, 2051.
- Schreurs, M.; Gooijer, C.; Velthorst, N. *Fresenius J. Anal. Chem.* **1991**, *339*, 499.
- Böttcher, C. J. F. *Theory of Electric Polarization. Volume 1. Dielectrics in Static Fields*; Elsevier Scientific Publishing Company: Amsterdam, 1973.
- Webb, S. P.; Phillips, L. A.; Yeb, S. W.; Tolbert, L. M.; Clark, J. H. *J. Phys. Chem.* **1986**, *90*, 5154.
- Kamlet, M. J.; Doherty, R.; Taft, R. W.; Abraham, M. H. *J. Am. Chem. Soc.* **1983**, *105*, 6741.
- Scheiner, S. *J. Phys. Chem. A* **2000**, *104*, 5898.
- Joshi, H. C.; Gooijer, C.; van der Zwan, G. *J. Fluoresc.*, submitted for publication.
- Boscá, F.; Cuquerella, M. C.; Martin, M. L.; Miranda, M. A. *Photochem. Photobiol.* **2001**, *73*, 463.
- Parker, C. A. *Photoluminescence of Solutions*; Elsevier: Amsterdam, 1968.
- O'Connor, D. V.; Phillips, D. *Time Correlated Single Photon Counting*; Academic Press: London, 1984.
- Kamlet, M. J.; Abboud, J.-L.; Abraham, M. H.; Taft, R. W. *J. Org. Chem.* **1983**, *48*, 2877.
- Reichardt, C. *Solvent and Solvent Effects in Organic Chemistry*; VCH Verlagsgesellschaft: Weinheim, Germany, 1988.
- Kosower, E. M. *J. Am. Chem. Soc.* **1958**, *80*, 3253.
- Kosower, E. M. *J. Am. Chem. Soc.* **1958**, *80*, 3261.
- Catalán, J.; Diaz, C.; García-Blanco, F. *J. Org. Chem.* **2001**, *66*, 5846.
- Marcus, Y. R. *Soc. Chem. Perkin Trans. 2* **1994**, *5*, 1751.
- Wilkinson, F.; Abdel-Shafi, A. A. *J. Phys. Chem. A* **1991**, *103*, 5425.
- Jellema, R.; Bulthuis, J.; van der Zwan, G.; Somsen, G. *J. Chem. Soc., Faraday Trans. 1* **1996**, *92*, 2563.
- Jellema, R.; Bulthuis, J.; van der Zwan, G. *J. Mol. Liq.* **1997**, *74*, 179.
- Solntsev, K. M.; Huppert, D.; Agmon, N.; Tolbert, L. M. *J. Phys. Chem. A* **2000**, *104*, 4658.
- Lee, J.; Robinson, G. W. *J. Am. Chem. Soc.* **1985**, *107*, 6153.
- Lee, J.; Griffin, R. D.; Robinson, G. W. *J. Chem. Phys.* **1985**, *82*, 4920.
- Robinson, G. W.; Thistlethwaite, P. J.; Lee, J. *J. Phys. Chem.* **1986**, *90*, 4224.
- Yuan, D.; Brown, R. G. *J. Phys. Chem. A* **1997**, *101*, 3461.
- Mashimo, S.; Umehara, T.; Redlin, H. *J. Chem. Phys.* **1991**, *95*, 6257.